



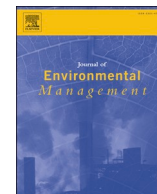
## **How effective is the retention of microplastics in horizontal flow sand filters treating stormwater?**

Downloaded from: <https://research.chalmers.se>, 2025-12-05 01:47 UTC

Citation for the original published paper (version of record):

Rullander, G., Lorenz, C., Herbert, R. et al (2023). How effective is the retention of microplastics in horizontal flow sand filters treating stormwater?. *Journal of Environmental Management*, 344.  
<http://dx.doi.org/10.1016/j.jenvman.2023.118690>

N.B. When citing this work, cite the original published paper.



## Research article

## How effective is the retention of microplastics in horizontal flow sand filters treating stormwater?

Gabriella Rullander<sup>a,\*</sup>, Claudia Lorenz<sup>c</sup>, Roger B. Herbert<sup>a</sup>, Ann-Margret Strömwall<sup>b</sup>,  
Jes Vollertsen<sup>c</sup>, Sahar S. Dalahmeh<sup>a</sup>

<sup>a</sup> Department of Earth Sciences, Uppsala University, Villavägen 16, SE-752 36, Sweden

<sup>b</sup> Water Environment Technology, Department of Architecture and Civil Engineering, Chalmers University of Technology, SE-412 96, Gothenburg, Sweden

<sup>c</sup> Aalborg University, Department of The Built Environment, Thomas Manns Vej 23, 9220, Aalborg Øst, Denmark



## ARTICLE INFO

Handling Editor: Jason Michael Evans

## Keywords:

Agglomeration  
Lab-scale experiment  
Microplastics  
Porous media filtration  
Stormwater pollution  
μ-FTIR analysis

## ABSTRACT

Microplastics accumulate in stormwater and can ultimately enter freshwater recipients, and pose a serious risk to aquatic life. This study investigated the effectiveness of lab-scale horizontal flow sand filters of differing lengths (25, 50 and 100 cm) in retaining four types of thermoplastic microplastics commonly occurring in stormwater runoff (polyamide, polyethylene, polypropylene, and polyethylene terephthalate). Despite the differences in particle shape, size and density, the study revealed that more than 98% of the spiked microplastics were retained in all filters, with a slightly increased removal with increased filter length. At a flow rate of 1 mL/min and after one week of operation, 62–84% of the added microplastics agglomerated in the first 2 cm of the filters. The agglomerated microplastics included 96% of high-density fibers. Larger-sized particles were retained in the sand media, while microplastics smaller than 50 μm were more often detected in the effluent. Microplastics were quantified and identified using imaging based micro Fourier Transform Infrared Spectroscopy. The efficient retention of microplastics in low-flow horizontal sand filters, demonstrated by the results, highlights their potential importance for stormwater management. This retention is facilitated by various factors, including microplastic agglomeration, particle sedimentation of heavy fibers and favorable particle-to-media size ratios.

## 1. Introduction

The limited circular economy in the plastics industry coupled with a high demand for plastics has generated large quantities of waste and resulted in microplastic (MP) pollution of the environment (Kershaw, 2016). The widespread pollution and the extensive persistence of MPs found in the environment have led to diverse effects on aquatic organisms, which is reason for concern (Amelia et al., 2021; Auta et al., 2017; Windsor et al., 2019). Entanglement and ingestion of MPs are common concerns for the health of aquatic life. In addition, plastic products (e.g. medical equipment, building materials and packaging) can contain additives, like phthalates, which can leach from MPs and prove toxic to organisms (Vinay et al., 2023). At the same time, organic and inorganic pollutants can sorb to MPs, making them a potential vector for spreading contaminants in the environment. There is also a potential risk for MPs to accumulate at higher trophic levels in the food web (Kumar et al., 2020).

MPs refer to plastic particles smaller than 5 mm (Thompson et al.,

2004), and are commonly divided into primary and secondary MPs where primary MPs are intentionally engineered particles, sometimes linked to pellet production, intended as abrasives in cosmetics and personal care products, or as synthetic fibers in the textile industry (Igalavithana et al., 2022). Secondary MPs are created through weathering and fragmentation of larger plastic debris, e.g. plastic debris left in the environment as a consequence of insufficient waste management (Fendall and Sewell, 2009; Hartmann et al., 2019). MPs can also be re-introduced into the environment through the application of sewage sludge, as farmland fertilizer (Igalavithana et al., 2022). MPs found in the environment can therefore have different shapes, e.g. fibers, spheres, fragments, and films, and particle counts tend to increase with decreasing particle size (Enders et al., 2015; Hartmann et al., 2019).

In aquatic environments, MPs often originate from land-based sources, i.e. those associated with treated wastewater discharge, industrial wastewater effluents, and urban stormwater runoff (Yano et al., 2021). In combined sewers, stormwater and wastewater are conveyed in the same pipe where the mixed water types are transported and treated

\* Corresponding author.

E-mail address: [gabriella.rullander@geo.uu.se](mailto:gabriella.rullander@geo.uu.se) (G. Rullander).

<https://doi.org/10.1016/j.jenvman.2023.118690>

Received 25 May 2023; Received in revised form 10 July 2023; Accepted 25 July 2023

0301-4797/© 2023 The Authors. Published by Elsevier Ltd. This is an open access article under the CC BY license (<http://creativecommons.org/licenses/by/4.0/>).

in wastewater treatment plants (WWTPs). However, in most cases, stormwater is conveyed in separate distribution pipes, and are often discharged into the environment without prior treatment (Österlund et al., 2023). This is an environmental issue, since high concentrations of MPs have been analyzed in stormwater runoff (Liu et al., 2019; Olesen et al., 2019; Smyth et al., 2021), which often contains polypropylene (PP), polyethylene (PE), polyamide (PA), polyethylene terephthalate (PET), polystyrene (PS) and polyvinyl chloride (PVC) with fragments and fibers as the dominant morphology (Chen et al., 2020; Mohamed Nor and Obbard, 2014; Molazadeh et al., 2023; Smyth et al., 2021; Werbowski et al., 2021). When analyzing MP content from environmental samples, visual inspection is commonly used, but there is a concern for inaccurate results, especially for smaller MPs (Löder et al., 2015; Simon et al., 2018; Tagg et al., 2015). In this study, we utilize micro Fourier Transform Infrared Spectroscopy ( $\mu$ -FTIR) imaging to analyze MPs, thus providing an opportunity to chemically identify and count smaller-sized MPs in a more time-efficient and strategic way (Mintenig et al., 2017). Additionally,  $\mu$ FTIR imaging provides particle size information derived from the chemical images (Tagg et al., 2020).

Polluted water from various sources is commonly treated by filtration-based techniques, where the water passes a porous media (Davis et al., 2009; Smyth et al., 2021), such as conventional rapid sand filters (RSFs) in WWTPs (Talvitie et al., 2017). In general, WWTPs have shown MP removal rates as high as 98–99% (Simon et al., 2018; Rasmussen et al., 2021; Gatidou et al., 2019). In cases where stormwater management is applied before its release into the environment, filtration-based techniques such as bioretention cells/rain gardens and constructed wetlands are also utilized, although the treatment systems are less advanced than that of full-scale treatment plants and often focus on self-sufficient, easily-constructed filtration units (Morash et al., 2019; Tirpak et al., 2021). In bioretention cells, pollutants can be removed through combinations of physical, chemical and biological processes. Primarily, suspended solids are retained through physical processes of sedimentation and filtration (Hatt et al., 2009; Payne et al., 2015). To remove suspended solids, metals and hydrocarbons in the systems, infiltration rates  $<0.04$  mm/s are often adapted. But, to further enhance removal of nitrogen, phosphorous, and pathogens infiltration rates as low as  $0.007$ – $0.014$  mm/s are recommended (Hunt et al., 2012).

A few field studies have been conducted to determine the removal efficiency of MPs from stormwater utilizing filtration techniques (Gilbreath et al., 2019; Kuoppamäki et al., 2021; Lange et al., 2021, 2022; Smyth et al., 2021; Werbowski et al., 2021), with results reflecting a MP removal efficiency of 70–100%. While these bioretention cells were not specifically designed for MP retention, the filtration units in Gilbreath et al. (2019) and Smyth et al. (2021) effectively removed MPs larger than  $125$   $\mu$ m and  $106$   $\mu$ m, respectively. Yet, it is established that MP abundance tends to increase as MP sizes decrease (Covernton et al., 2019). Indeed, Lange et al. (2022) identified an abundance of  $20$ – $100$   $\mu$ m MP in stormwater runoff, albeit with varying concentrations. The authors also found that vegetated bioretention cells exhibit greater retention of smaller sized MPs compared to non-vegetated filters, attributed to the smaller pore size provided by introducing a substrate layer. Although the available studies showcase promising results for MP removal, it is important to acknowledge that the MP sizes analyzed may not be inclusive enough, and that the aim of these studies was primarily to quantify and characterize MPs in stormwater. As such, detailed discussion on MP removal and the factors affecting it, e.g. particle density and shape, was not extensively explored. At the same time, filtration units are often, but not exclusively, designed for the vertical percolation of water (Choi et al., 2021; Samuel et al., 2012). Horizontal flow filters are sometimes favored due to less excavation work and constraints on filter lengths (Adugna et al., 2017; Nkwonta, 2010), but field studies on MP retention in such systems are limited.

Previous lab-scale studies have investigated the retention of MPs in porous media, but there is not yet a consensus on the impact of MP characteristics on the degree of MP retention. For example, Sembiring

et al. (2021) constructed an RSF experiment to study the removal of fragmented plastic bags and tire particles ( $10$ – $500$   $\mu$ m) in vertical continuous down-flow columns ( $L = 100$  cm,  $D = 10$  cm) with silica sand ( $0.35$ – $0.70$  mm). The set-up included coagulation and pre-sedimentation to simulate a treatment plant, which generated removal rates of over 90% for each fragment type. Similarly, Dong et al. (2021) found a low mass recovery of PET fragments ( $0.25$ – $5$   $\mu$ m) in down-flow vertical columns with quartz sand ( $0.35$ – $0.4$  mm) and attributed the retention to shape and high particle density. However, Tumwet et al. (2022) were able to correlate a decrease in MP retention with smaller-sized MPs and fragment shapes by investigating PVC fragments and PE spheres ( $125$ – $300$   $\mu$ m) in continuous up-flow vertical columns with quartz sand ( $1.6$ – $2.9$  mm). Studies regarding horizontal flow filters are less common, but Chen et al. (2021) investigated MP retention of larger-sized fibers and fragments ( $0.5$ – $4$  mm) in microcosm subsurface constructed wetlands, and found that the microcosms could fully retain MPs through physical filtration, where the particles accumulated in the proximity of the microcosms' inlets (Dong et al., 2021; Sembiring et al., 2021).

Most studies agree that MP mobility in porous media often correlates to the size of MPs; i.e. increased mobility with decreased MP size (O'Connor et al., 2019; Zhang et al., 2022). Still, the significance of MP characteristics is uncertain, and the outcomes of horizontal flow experiments remain unknown. Additionally, most experiments regarding MP transport in porous media focus on the discrete mobility of MPs. Under natural environmental conditions, it is likely that numerous types of MP of differing sizes, shapes, and densities co-occur in the same environment and affect the mobility of each other. To address these knowledge gaps, the retention of heterogenous thermoplastics commonly occurring in stormwater was investigated in lab-scale horizontal flow sand filters. In short, a mixture of PA, PE, PP, and PET particles with different shapes and sizes was spiked in filters of various length and the accumulated effluents and sand media were analyzed for MPs after one week of operation. Specifically, we investigated (i) the overall retention of MPs in horizontal flow sand filters, (ii) the effects of filter length ( $25$ ,  $50$  and  $100$  cm) on MP retention, and (iii) the retention behavior of MPs in response to differing sizes, densities and shapes. Based on our current knowledge, this is the first study aimed to presents insights into filtration efficiency by examining retention of MPs under horizontal flow, while focusing on a diverse range of MPs often associated with stormwater runoff, with the goal of enhancing and developing effective filtration strategies.

## 2. Method and materials

### 2.1. Porous media

Sand was used as a porous media in the horizontal flow filters (Natural sand,  $1$ – $3$  mm, Hasselfors) and consisted primarily of quartz and feldspars. The particle distribution curve of the sand was determined, indicating well-graded sand where 50% of the sand grains were between  $1$  and  $1.9$  mm (see also Supplementary Information S1). Additionally, the sand had a pH of  $7.9$ , when shaken with deionized water, and contained  $0.2\%$  volatile solids.

### 2.2. Microplastics

A mixture of thermoplastic MPs was used in the study and was comprised of spherical particles of PA ( $25$ – $30$   $\mu$ m) and ultra-high molecular weight PE (UHMWPE), referred to as PE ( $125$   $\mu$ m), fibers of PP (length:  $241 \pm 340$   $\mu$ m, width:  $28$   $\mu$ m) and PET (length:  $291 \pm 224$   $\mu$ m, width:  $23$   $\mu$ m), and fragments of PP, referred to as PPblixter ( $63$   $\mu$ m  $\pm$   $53$ ), all with different densities (PA:  $1.020$  g/cm<sup>3</sup>, PE:  $0.94$  g/cm<sup>3</sup>, PP:  $0.90$  g/cm<sup>3</sup>, PET  $1.35$  g/cm<sup>3</sup>). To obtain the MP mixture,  $0.1$  g each of PA, PE, PPblixter, PP and PET fibers were homogenously mixed in a glass beaker. The spherical MPs were purchased ready-made and

fragments and fibers were obtained by cutting and shredding larger items (for further information see Supplementary Information S2 and S3). The size distribution of the MPs was analyzed using  $\mu$ FTIR imaging and the MPs were visualized by field emission Scanning Electron Microscopy (SEM, Zeiss Supra 35-VP microscope, Carl Zeiss SMT, Oberkochen, Germany; see Fig. 1).

### 2.3. Horizontal flow sand filter set-ups

The horizontal flow sand filter experiments were run with filter set-ups (S) of three defined lengths of 25, 50, and 100 cm. For each length, three horizontal sand filter set-ups (S1, S2, and S3) were constructed using polyvinyl chloride (PVC) pipes with an inner diameter of 4.6 cm (Fig. 2). Hence, 9 columns in total were studied. S1 and S2 were spiked with the MP mixture and the retention of MPs was evaluated for the different filter lengths. S3 served as an experimental control, and was therefore not spiked with any MPs. All set-ups were filled with sand, and packed manually through a free-falling technique. Due to the use of PVC in the experimental setups, retention of PVC MPs was excluded from the study.

The total weight of the packed set-ups was noted and the porosities of the filters were estimated based on sand particle density, the weight of added material, and the volume of filter lengths (Larsson, 2008, Table 1). To acclimatize and wash away potential background contamination, the sand packed in the set-ups was flushed with tap water, over a period of one week. The rinsing water was supplied using a peristaltic pump connected to silicon tubes (Masterflex L/S Labinette, Sweden), at a flow rate of 1 mL/min. The theoretical residence time of the filters was determined for S3 by estimating the quotient of filter pore volume (PV; the pore volume of sand media and water volume at the ends of the column) and system flow rate (Q; see Eq (1) and Table 1).

$$\text{Residence time}_T = \frac{PV}{Q} \quad (1)$$

### 2.4. Microplastic spiking, water pumping, and sample collection

Using a metal spoon, a 1 cm deep depression was made in the filter inlets of S1 and S2, in which the MP mixture was added and then covered with sand, referred to as “the MP-mixing zone”. After spiking the filters with the MP mixture, they were fed with tap water at a continuous flow of 1 mL/min using a peristaltic pump (Masterflex L/S Labinette, Sweden). Considering the area of the filter inlet (A), the infiltration rate (Q/A) was 0.01 mm/s, which was within the guidelines of infiltration rates (0.007–0.014 mm/s) often shown to enhance removal of nitrogen, thermal pollution, phosphorous and some

pathogens in stormwater filtration units (Hunt et al., 2012). The filters were fed with tap water for one week and the accumulated volume of each filter was collected in glass jars, resulting in a total volume of approx. 10 L per filter.

### 2.5. Microplastic extraction

The MPs exiting the filter or retained in S1, S2, and S3 were extracted through filtration and density separation techniques. The MPs exiting the filters (referred to as “effluent”) of S1, S2, and S3 were extracted by percolating the water through 10  $\mu$ m stainless steel filters, applying vacuum filtration. The inner walls of the filtration unit were thoroughly rinsed with deionized water to minimize loss of MPs and cross-contamination. The MPs retained in the sand of S1 and S2 were extracted from two sections of the filters: (1) the MPs agglomerated near filter inlet, referred to as “MP-mixing zone”, (2) MPs retained in the sand of the remaining lengths (i.e. MPs found 2–25, 2–50, and 2–100 cm) referred to as “sand media”. The agglomerated MPs were removed carefully from the filter inlet using a metal spoon and the remaining sand in filter lengths (2–25, 2–50, and 2–100 cm) was emptied into glass jars and oven-dried at 40 °C, until dry weights had stabilized.

To separate the MPs from the sand media fraction, the separation method of Masura et al. (2015) was applied, but with some modification as follows: In a glass jar, a dense salt solution composed of 1.4 g/cm<sup>3</sup> ZnCl<sub>2</sub> was added to the sand media at a ratio of 1 mL solution to 1 g of sand. The density of the ZnCl<sub>2</sub> solution allowed even the heavy PET fibers to float. The sand and salt solutions were stirred vigorously for 5 min using a metal spoon and then left for 24 h to allow the flotation of MPs and sedimentation of the sand. After 24 h, the supernatants were transferred to individual 400 mL separatory funnels using an ALTEA-XV peristaltic pump (SPW industrial, USA) with a 6 mm silicon tube. The pump's silicon tube was flushed with smaller volumes of deionized water after usage, with the rinsed water transferred to each corresponding funnel. This procedure was repeated until no visual MPs could be seen in the supernatant. Afterwards, all remaining liquid in the glass jar was transferred to the separation funnels. The first fraction, the agglomeration, was transferred directly to separatory funnels where the same density liquid (ZnCl<sub>2</sub>, 1.4 g/cm<sup>3</sup>) was added (Masura et al., 2015). The density liquid in the separation funnels measured two thirds of the funnel volumes and was adjusted when needed. The liquids were left to settle for 24 h, after which the settled inorganic materials were discarded from the bottom valve of the funnels. This procedure was repeated until there was no visible settling of materials in the funnels. The remaining supernatants were collected and vacuum filtered on 10  $\mu$ m stainless-steel filters. The sand media from the total filter lengths,

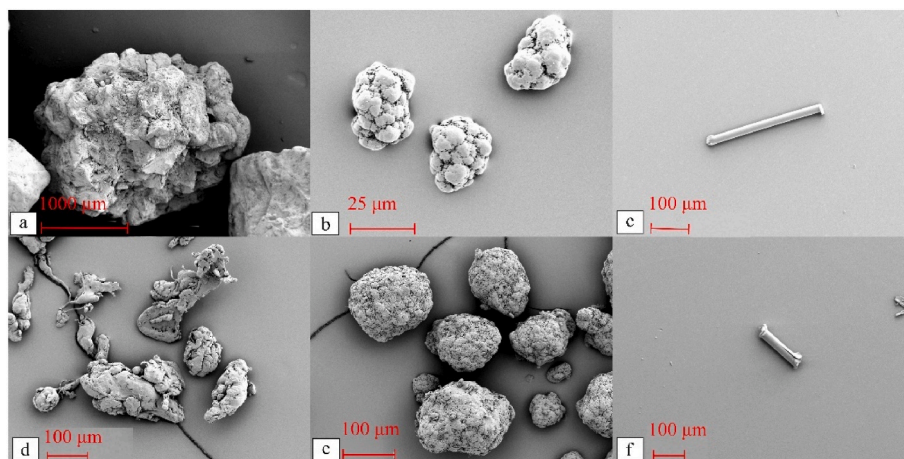


**Fig. 1.** Scanning Electron Microscope (SEM) images of MPs and the sand used in the study. a) Sand grain b) spherical PA c) PET fibers d) PPblixter e) PE and f) PP fibers.



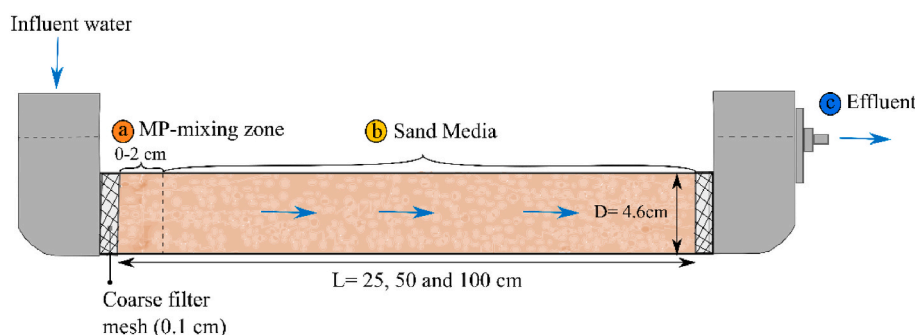


**Fig. 2.** Horizontal flow filter set-up established for three filter lengths ( $L = 25, 50$ , and  $100$  cm). The MP mixture was deposited  $1$  cm to the right of the metal filter mesh in the inflow direction of the filter, referred to as the “MP-mixing zone”. MP numbers and types were identified in three sections of the filter as follows: a) the MPs agglomerated in the “MP-mixing zone” ( $0$ – $2$  cm) of the filter b) MPs retained in the sand in the remaining lengths ( $2$ – $25$ ,  $2$ – $50$ , and  $2$ – $100$  cm) of the filter, referred to as “sand media” and c) MPs found in filter outlets, referred to as “effluent”.

**Table 1**

Physical and hydraulic properties of the sand filters, including volumes, sand mass, porosities, pore volume (PV) and theoretical residence time.

	Filter properties		
Filter length (cm)	25	50	100
Mass of sand (g)	522	1192	2576
Total filter volume ( $V_t$ ; $\text{cm}^3$ )	377	830	1636
Porosity ( $f$ ; %)	43	43	43
Pore volume (PV; $\text{cm}^3$ )	163	357	704
Theoretical residence time (min)	869	1070	1430

$0$ – $25$ ,  $0$ – $50$ , and  $0$ – $100$  cm from S3, was processed as the sand media of S1 and S2, to account for background contamination of MPs in the original sand media.

All stainless-steel filters containing extracted MPs were transferred to individual glass beakers where pure ethanol was added until the metal filters were fully submerged. The beakers were then covered with aluminum foil and sonicated for  $15$  min to detach MPs from the metal filters. After sonication, the filters were removed from the beaker and rinsed three times with pure ethanol. The collected MP-ethanol suspensions were transferred to  $20$  mL glass vials, adjusted to a fixed volume and stored at fridge temperatures ( $4$  °C).

## 2.6. Microplastic identification and quantification

The concentrated MP-ethanol suspensions were homogenized using a vortex stirrer (VWR,  $60$  s), and  $0.1$ – $10\%$  of the total sample was deposited on  $13 \times 2$  mm zinc selenide optical windows (Crystran, UK) mounted in a micro compression cell (Pike Technologies, USA). The number and chemical composition of MPs deposited on windows were determined using a Cary 620 FTIR Focal Plane Array (FPA) microscope coupled with a Cary 660 IR spectrometer (Agilent Technologies, USA). The microscope was equipped with a  $15\times$  Cassegrain objective and a  $64 \times 64$  FPA detector with a  $5.5$   $\mu\text{m}$  pixel resolution. The complete area of the window was analyzed in transmission mode. All samples were scanned with spectral ranges appropriate for MP analyses,  $3750$ – $950$   $\text{cm}^{-1}$ , at  $8$   $\text{cm}^{-1}$  resolution with  $16$ -coadded scans (Olesen et al., 2019; Simon et al., 2018).

The imaging spectra were further processed in the siMPle v.1.3.1 $\beta$  (Systematic Identification of MicroPlastics in the Environment) freeware (Primpke et al., 2020). The freeware allows for semi-automated matching of sample spectra with a spectra reference library (Primpke et al., 2017, 2018). In this study, Aalborg University provided the reference spectra library, which contained spectra of various standard plastics and organic materials (Vianello et al., 2019). Additionally, the spectra obtained for the standard MPs used in the experiment were added to the reference library. To identify the MPs, first siMPle matches the measured spectrum and its 1st derivative with that of the reference spectrum, and then it scores the match based on the correlation between the spectra. A 1st and 2nd threshold were set by the operator, which influence core and adjacent pixel matches with the reference library

(Vianello et al., 2019; see also Supplementary Information S4). The output from the siMPle freeware were types of MPs identified in the samples, the number of particles identified for each MP type, estimates of particle length (the longest distance between identified MP pixels) and width (the minimum distance between two boundary points of a particle), also known as the Feret minor diameter.

## 2.7. Contamination control

Jars, filter disks, beakers, and petri dishes used in the experiment were made either of metal or glass. Vinyl gloves, fume hoods, and cotton lab coats were used during MP extraction. To minimize the deposition of MPs from air in media, the inlet and outlet of the filters were covered with aluminum foil during the entire period of the experiment. To evaluate the atmospheric deposition of MPs in the laboratory, a glass beaker with an inner dimension of  $4.5$  cm was filled with  $100$  mL tap water and placed alongside the filters for the duration of the experiment. The possible contamination from the silicone tubes and tap water was determined by pumping tap water ( $7$  L) through tubes using the peristaltic pump and then analyzing the potential MP content in the water. Also, parallel with S1 and S2 set-ups, an identical control set-up S3, without MP spiking, was run to measure potential background contamination associated with the sand media.

## 2.8. Data and statistical analysis

The number of MPs found in the effluents of control (S3) was subtracted from MP numbers of S1 and S2 effluents for each MP type found in the respective filter length. Since the MP mixture in the experiments included PP of two different shapes (fibers and fragment), the elongation factor was utilized to differentiate between fragments and fibers, where PPs with elongation ratios larger than three were sorted as fibers and the remaining MPs as PPblixter (Hartmann et al., 2019; Lusher et al., 2020; Martínez Silva and Nanny, 2020; Vianello et al., 2019).

A binary-decision tree with an interaction-curvature algorithm was fitted for all MPs, to estimate how significant certain characteristic variables were for accurate prediction of MP transport. The predictor importance refers to how the features influence tree splits, in order to accurately predict MPs found in the effluents. The features included one categorical predictor of MP type (PA, PE, PPblixter, PP, and PET), and four continuous predictors representing MP length and width, particle densities, and filter lengths (Rokach and Maimon, 2005). The predictor importance values were given by summing the changes in the risk associated with each predictor and dividing the sum by the number of nodes on the branch (Breiman, 1984). All data was processed in MATLAB R2021a.

### 3. Results & discussion

#### 3.1. Retention of microplastics

Analysis of the sand media in the control set-up (S3) revealed the presence of PP, PET, and PE particles. At the same time, analysis of atmospheric deposition and tap water also contained PE, PP, and PA particles. Thus, the MPs found in the effluents of the control could be due to contamination from the sand media, atmospheric deposition, or cross-contamination. S3 effluents contained PP, PE, PET, and PA MPs in decreasing order (For further details view Supplementary Information S5); as described previously, the analytical results from S1 and S2 have been corrected for MPs detected in the control set-up S3.

The quantification and identification of MPs were derived from extrapolation of the analysis of 0.1–10% of sample volumes. The aliquots of the smallest sub-samples, 0.1%, allowed the identification of around 500–2900 MPs per sample from sand media and MP-mixing zone; the analysis of effluent sub-samples, 10%, provided 20–160 identified MPs per sample. A vast number of MPs was counted in the total retention (i.e. the sum of MPs in MP-mixing zone and sand media) in comparison to total number of MPs in the effluents (see also Supplementary Information S6).

The horizontal flow sand filter set-ups retained over 99% of total MPs for all filter lengths (Fig. 3a). The method of spiking MPs in the mixing zone caused MPs to agglomerate and 62–85% of the initial MPs therefore remained in the MP-mixing zone (the first 2 cm of the filter) and to a lesser extent, 18–38%, in the remaining 2–25, 2–50, and 2–100 cm of the sand media (Fig. 3a). Of all MPs found in the MP-mixing zone and sand media across all set-ups and filter lengths, 16% were fibers. In contrast, only 10% of MPs in effluent were fibers. This can be seen from the increased elongation factors for particles in the sand media and MP-mixing zone fraction of the set-ups, where most fibers have lengths larger than 100  $\mu\text{m}$  (Fig. 3b).

The individual removal was larger than 99% for all MP types in each set-up and filter length, except for PE particles in set up 2 with 25 cm filters, where 2.3% PE MPs was found in the effluent (Fig. 4). Interestingly, PET fibers were retained completely, 100%, by most filters, whereas PP fibers were seen in most effluents, still with a high relative percentual removal ranging from 99.8 to 100%. It should be mentioned that PA particles were present in all effluents, possibly as a result of their smaller size (25–30  $\mu\text{m}$ ) and spherical shape, which have facilitated

transport through the filters (Fig. 4).

#### 3.2. Distribution and relative abundance of microplastics

The two fiber types in the experiment displayed differing distribution and abundance in the horizontal sand flow set-ups. A large percentage of high-density PET fibers, over 96%, was identified in the MP-mixing zone in all set-ups and filter lengths. Lower-density PP fibers were also identified in the MP-mixing zone but were the dominant fibers type in sand media and effluents (Fig. 5). Previous research has linked an increase in MP and colloid densities to an increased mobility in vertical columns (Chrysikopoulos and Syngouna, 2014; Koutnik et al., 2022a). In this study, the opposite was found and large PET fibers were almost completely retained in the MP mixing zone (Fig. 5). This was also found for lab-scale constructed subsurface flow wetlands, where most fibers were retained near system inlets (Chen et al., 2021).

For the spherical particles, PA represented the largest relative abundance of total MP particles in the MP-mixing zone, whereas the relative abundance of PE particles was more significant in the sand media (Fig. 5). Generally, when pooling all filter lengths of the set-ups, 77% of PA was confined in the MP-mixing zone, whereas 63% of PE particles were retained in the sand media of the remaining filter lengths. The fragments, PPblaxter, constituted similar relative MP ratios in the MP-mixing zone and sand media for all set-ups and filter lengths (Fig. 5).

#### 3.3. Effects of microplastic characteristics on particle retention and transport

The current study utilized MPs with wide size ranges and shapes, starting from 25  $\mu\text{m}$  and included spheres, fragments and fibers. The literature suggests that the retention of particles larger than 10  $\mu\text{m}$  in porous media are dominated by hydrodynamics, gravity and inertial effects (Frey et al., 1999; Gohr et al., 1999), where the flow and movement of a fluid, the force of gravity acting on particles and the tendency of particles to transport in their trajectory affects their potential retention. It is also argued that settling and interception are the main retention mechanisms for particles of these sizes (Yao et al., 1971). Although physio-chemical interactions mainly govern the retention of much smaller particles than what has been used in this study, the hydrophobic nature of the studied MPs should be mentioned as a potential influence on retention through hydrophobic interactions (Hou et al.,

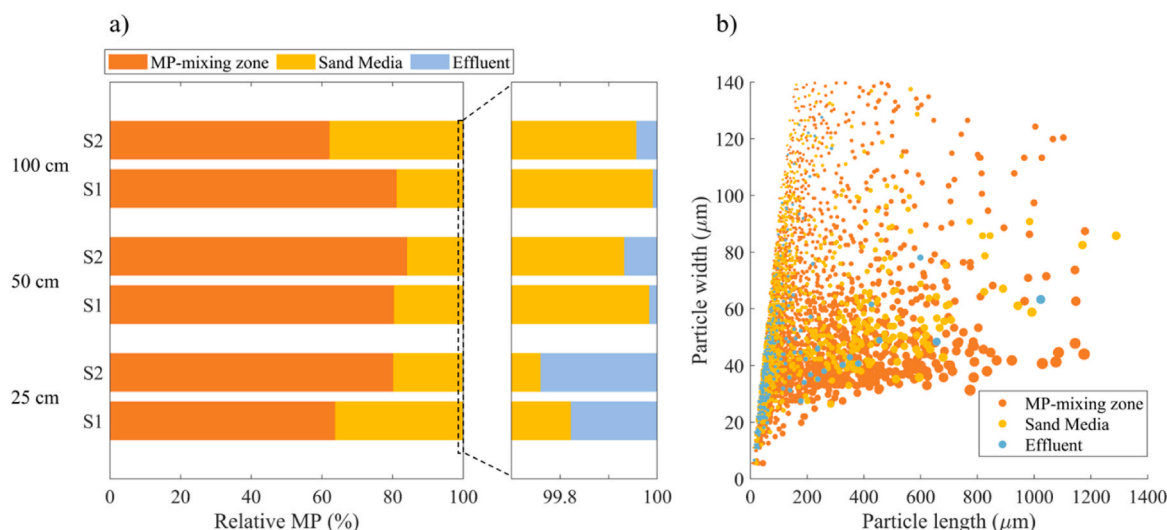


**Fig. 3.** The fate of MPs in the horizontal flow sand filters. a) Percentual distribution of MPs quantified in MP-mixing zone, sand media, and effluent for set-up 1 and 2 (S1 and S2) and each filter length (25, 50 and 100 cm), where relative MP (%) is given by dividing the number of MPs found in a section of the filter with all MPs associated with the filter length. b) Width and length dimensions for MPs in MP-mixing zone, sand media, and effluent, combined for all set-ups and filter lengths. The dots are sized according to the particle elongation factor, with increasing size for increased elongation. Note the scale difference in the X and Y axes.

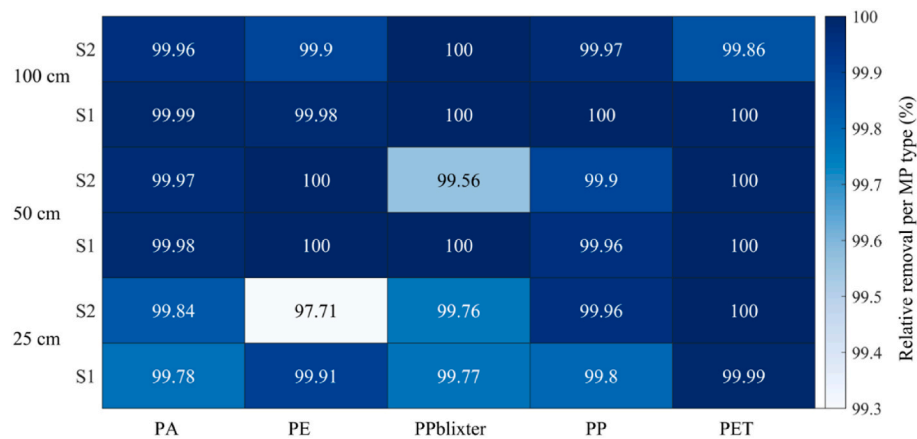


**Fig. 4.** A heatmap of the percentual relative removal of the individual MP types in each set-up and filter length, showing the fate of MPs in the horizontal flow sand filters where darker colors represent increased percentual removal. S1 and S2 denote the replicates of the experimental set-ups 1 and 2.

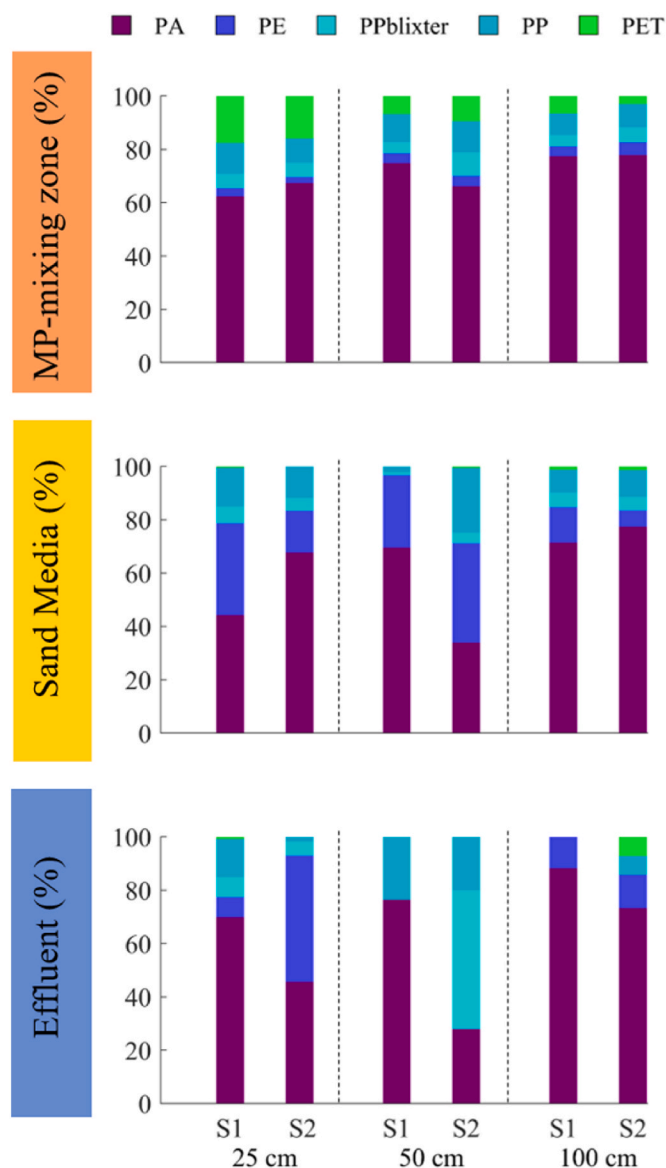


**Fig. 5.** Relative distribution of MP types counted in MP-mixing zone, sand media, and effluent of set-ups S1 and S2 (25, 50 and 100 cm). The percentages were estimated by dividing the MP counts of each MP type by the total counts of all MP types detected for the specific filter length.

2020).

This study utilized a constant horizontal flow to analyze MP retention in porous media. As such, we expect gravitational forces to have a larger effect on the retention of suspended particles compared to vertical systems, as the force is perpendicular to the general fluid movement (Chrysikopoulos and Syngouna, 2014; Yiantsios and Karabelas, 2003). However, the retention of MPs should be less influenced by gravity than other suspended particles due to their relatively low density. For example, the density of MPs utilized in the experiment ranged from 0.90 to 1.020 g/cm<sup>3</sup> for PP, PE and PA with only PET fibers providing a density higher than that of water 1.35 g/cm<sup>3</sup>. Indeed, high-density PET fibers were retained to a greater extent in filters compared to other MPs, most likely due to the influence of gravitational forces. This observation is also supported by Benamar et al. (2005) who compared the transport of PA MPs (25 µm, 1.04 g/cm<sup>3</sup>) with natural silt particles in porous media, and found that PA particles were retained to a lesser degree due to their limited sedimentation.

It should also be mentioned that flow and infiltration rates can influence the retention efficiency of particles in a porous media. For instance, Hou et al. (2020) found that the retention of PE MPs (40–48 µm) in vertical flow columns packed with quartz sand (1–2 mm and 2–4 mm) increased with a decreased infiltration rate, 0.02 mm/s, as the probability of contact between MPs and sand media increased. The current study was designed with a low infiltration rate, 0.01 mm/s, as such, the high MP retention found in this study (>98% for all studied MPs), is most likely favored by the low infiltration rate, and it is possible that the retention would have been even greater for higher density particles, as sedimentation dominates retention in low-flow systems (Ahfir et al., 2007).

Another critical factor determining retention in porous media is the ratio of sand media diameter,  $d_m$ , to suspended particle diameter  $d_p$ , ( $d_m:d_p$ ). For larger particles with ratios <10, mechanical removal and clogging of filter surfaces is expected, while much smaller particles providing ratios >1000 are predominantly retained through physical-chemical filtration (Sakthivadivel and University of California Berkeley., 1969). For example, Ahfir et al. (2017) studied the retention and transport of suspended particles in coarse sand columns with a  $d_m:d_p$  ratio around 36, at flow rates much larger than in the current study, and found that particles larger than 20 µm were completely retained by the porous media. In the present study, despite the low flow and infiltration rate, the smallest MP, PA (25–30 µm), was found in all effluents. This could be attributed to a larger  $d_m:d_p$  ratio around 68, and a lower particle density, compared to most suspended solids. It has also been suggested that the retention of particles can occur if the average particle diameter exceeds 5–10% of the media's average particle size (DeNovio et al., 2004; Porubcan and Xu, 2011). In this experiment, the average

particle size of the sand was 1.7 mm, which suggests that MPs larger than 85–170  $\mu\text{m}$  could be retained in the filters through physical filtration. Notably, 97% and 85% of all MPs counted in effluents had particle widths and lengths smaller than 100  $\mu\text{m}$  (Fig. 6). This aligns with previous research indicating that as MP sizes decrease, vertical and horizontal transport in soil and sand media tends to increase (Tumwet et al., 2022; Zhang et al., 2022). It is therefore not surprising that particle length and width were the most important factors for predicting MP retention, according to the decision tree (for further information see Supplementary Information S7).

Considering the influence of particle size on MP retention, the number of PE MPs identified in the effluent of a 25 cm filter was surprising, seeing the supplier's information about the average particle size (125  $\mu\text{m}$ ). However, FTIR imaging revealed that the PE particles had a wider size range than anticipated, which was also noticed from the SEM images (Fig. 1e; Fig. 6). Indeed, the portion of smaller-sized PE MPs, 25–50  $\mu\text{m}$ , could explain the horizontal transport in the 25 cm sand filter. Similarly, the transport of PP fibers found in this experiment is unexpected, given that their average particle lengths are larger than 100  $\mu\text{m}$  (Fig. 6). However, the characteristic shape of the PP fibers, with one dimension being considerably larger than the other and consistent widths (25–50  $\mu\text{m}$ ), may explain their transport (Fig. 6). This suggests that transport of PP fibers is possible, but that it ultimately depends on the fibers' particular orientation and movement during the experiment.

At the same time, fragments have been linked to lesser vertical mobility in column experiments, due to their tendency to entangle in porous media (O'Connor et al., 2019). However, this study identified PPblixter in the effluents of 25 and 50 cm filters. The preparation of PPblixter involved the use of strong mechanical forces, which may have caused invisible fractures and weakened some particles. While passing the filter media, the friction between the sand and the fragments could have further broken some PPblixter into smaller particles, making them more likely to be transported to the filter effluents.

It is also important to note that the porosity of a systems, in itself, does not govern the retention in filter-units. Narrow pore passages, cavities and cracks along with surface roughness of the media can increase retention of MPs by restricting or trapping MPs, depending on their size and shape. A wider grain-size distribution of the porous medium, with a mixture of larger and smaller grains, can contribute to increased retention as smaller sand particles can wedge between larger sand grains, and create such pore spaces. In this study the wider grain-size distribution may have contributed to the high (>98%) MP retention, as observed in the findings of Ahfir et al. (2017).

#### 3.4. Agglomeration of microplastic in the MP-mixing zone

Particle aggregation can occur when two particles collide and attach, a process that has been noticed for MPs in aquatic environments (Zhang,

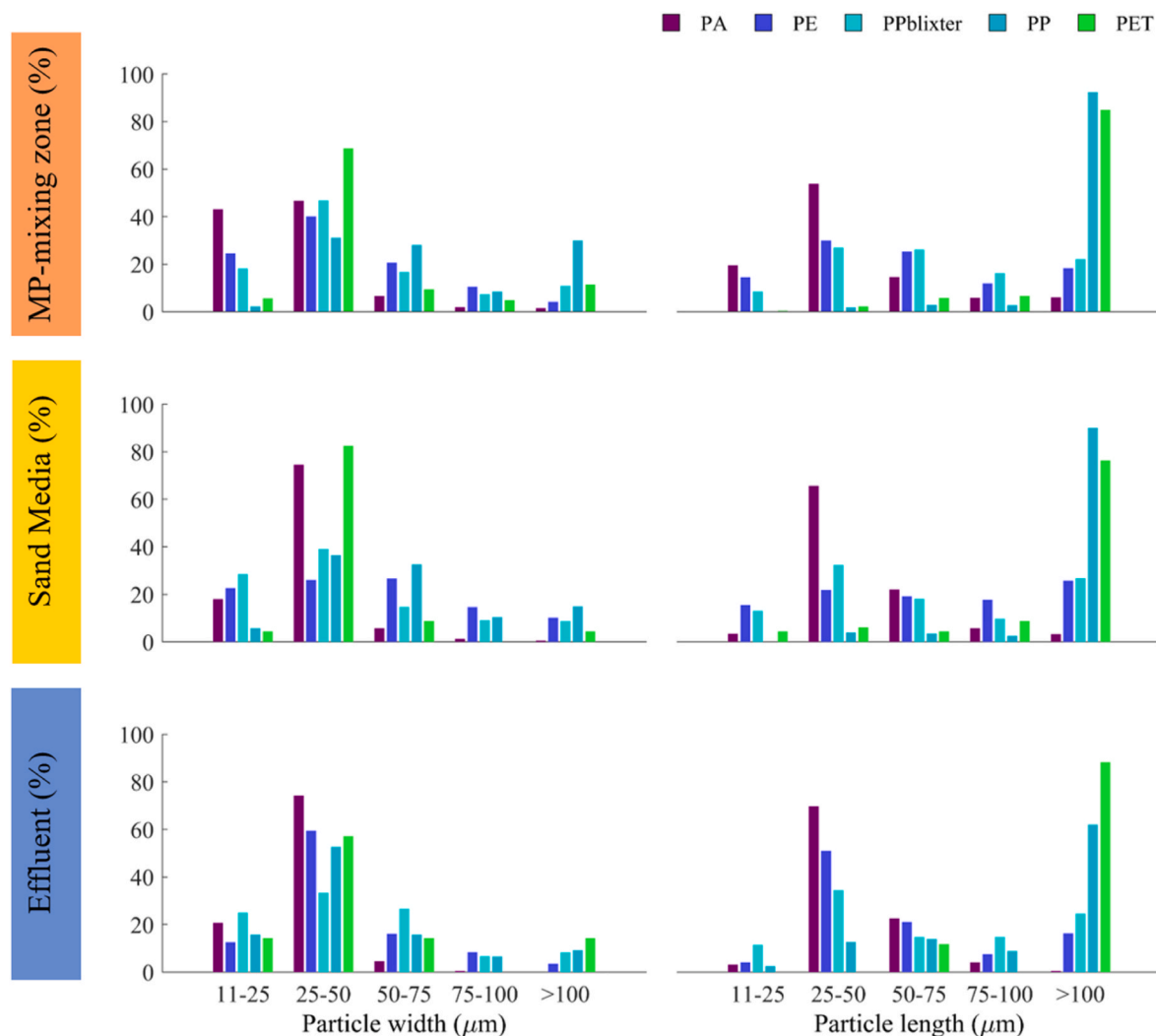


Fig. 6. Size distributions of MPs displaying the length and width distributions of individual MP types pooled from all set-ups in MP-mixing zone, sand media, and effluent, over 25  $\mu\text{m}$  intervals. Note that MP types reach 100% when combining their abundance over all intervals.



2014), a natural physio-chemical process influencing MP transport (Alimi et al., 2018; Wang et al., 2021). In the environment, MPs can aggregate with mutual MPs as homo-aggregates or with other particles and biota, creating hetero-aggregates (Long et al., 2017). This study's agglomeration consisted of MP aggregations between matching MPs and different MP types inclined to attach due to similar sizes and physico-chemical aspects like hydrophobicity (Rhein et al., 2022). MPs extracted from the MP-mixing zone underwent ultrasonic treatment prior to analysis, yet, homo-aggregation of PA larger than 250  $\mu\text{m}$  was noticed, considerably larger than the average size distribution of the individual PA particles ( $38.9 \pm 16 \mu\text{m}$ ) (Fig. 6). In general, aggregation is governed by MP characteristics (e.g., morphology, size, density), where smaller-sized MPs are more likely to aggregate than larger particles, often as a result of steric forces related to MP hydrophobicity (Drago et al., 2020; Kumar et al., 2021). Since all MPs in this experiment were larger than 10  $\mu\text{m}$ , it is expected that loosely-bound aggregates formed, which are more frequently affected by shear forces than by surface interactions (Hüffer et al., 2017). As such, it is expected that higher flow rates, with increased drag forces exerted on MPs, could have increased the MP transport from the agglomeration formed in the MP-mixing zone. The accumulation of larger sized MPs in filter inlets could also have impacted the movement of smaller MPs by creating a physical hindrance that compromised the flow of some MP types (e.g. PA), which could otherwise have been present in effluents (Sakthivadivel, 1969). Besides acting as a mechanical hindrance at the filter inlet, individual MP densities could be altered when aggregated to MPs of higher density, affecting the mobility of particles. The extent of homo-aggregation found in this experiment is likely to be negligible in stormwater runoff, as particle concentrations of the same plastic materials are considerably lower, with natural particles as the primarily content in stormwater runoff (Eitzen et al., 2019). However, the phenomenon of MP agglomeration could still be considered for terrestrial MP modeling, where MPs have accumulated over time.

### 3.5. Experimental restrictions and limitations

It is important to note that virgin MP particles utilized in this experiment differ from environmentally obtained MPs that have otherwise been subjected to aging and weathering in the environment. Stormwater filtration units may also provide differing retention capacities depending on influent water quality, but due to the novelty of MP studies regarding stormwater and sand media retention, the water source in this experiment was restricted to tap water. At the same time, the mass of spiked MPs used in this experiment is vastly exaggerated compared to concentrations found in stormwater sources but could represent MP numbers accumulating in filter units over many years (Koutnik et al., 2022b). The extensive feeding of MPs and the one-week operating time provided an exaggerated scenario to evaluate MP retention under extreme conditions.

## 4. Conclusions

This study examined the retention and transport behavior of mixed MP thermoplastics in horizontal flow sand filters with lengths 25, 50, and 100 cm. The study shows that the horizontal flow sand filters can effectively remove different types, shapes and sizes of MPs even in the shortest 25 cm filters (up to 98%) due to favorable particle-size to grain-size ratios, low infiltration rate and MP agglomeration in the MP-mixing zone. The length and width of the particles were found to be the most influential factors in determining MP retention in the experiment. The intentional spiking of high loads of MPs in the mixing zone resulted in a significant portion (62–85%) of MPs agglomerating and remaining in the MP-mixing zone. High density PET fibers (96%) were influenced by gravity forces and retained to the greatest extent in the MP-mixing zone, whereas a smaller portion of the lower density fibers (PP) was detected both in effluent and sand media. The smallest MP utilized in the

experiment (PA) was noticed in all effluents, attributed to its small-size and low-density. The lab-scale experiment demonstrated that horizontal flow sand filters are promising solutions for MP retention, even under extreme MP loads and operating conditions. In summary, this study provides promising results for the use of sand filter units to address the issue of MP pollution in stormwater management. Yet, further research is needed to assess horizontal flow filters for MPs removal under field conditions i.e. natural stormwater. Future experiments focusing on testing the performance of the filters at varying MP concentrations and with stormwater flows of different rainfall duration and intensity are needed to determine MP retention under real-world conditions.

### Author contribution statement

Gabriella Rullander conducted the experimental set-ups, lab experiments, and analysis and is the main author of the paper and responsible for all data visualization. Sahar Dalahmeh, Roger Herbert, Ann-Margaret Strömval, Claudia Lorenz and Jes Vollertsen contributed to the experimental design and methodology that produced the experimental results and paper, and co-supervised the Ph.D. fellow Gabriella Rullander. The first author collaborated with all secondary authors in editing, reviewing and discussing the results and writing of the manuscript. Sahar Dalahmeh is the project's founding acquisitioner and Gabriella Rullander's main supervisor. All authors have contributed to the research in a meaningful way.

### Funding sources

The work presented in this article is part of the activities implemented within the project "Cities with less microplastics: Road-side green filters to remove microplastics from urban stormwater", which was funded by the Swedish Research Council for Environment, Agricultural Sciences and Spatial Planning (FORMAS), grant number 2019-01911.

### Declaration of competing interest

The authors declare that they have no known competing financial or personal interests that could have influenced the work reported in this paper.

### Data availability

Data will be made available on request.

### Acknowledgements

We have greatly appreciated the assistance and expertise of PhD fellow Lucian Iordachescu at Department of the Built Environment-Aalborg University, for the help in introducing hands-on  $\mu$ -FTIR analysis and providing us with the reference library utilized in this experiment. We are also thankful for the expertise from the unit of campus management *Lagerträdet* at department of earth sciences- Uppsala University, for their efforts in preparing the filter setup.

### Appendix A. Supplementary data

Supplementary data to this article can be found online at <https://doi.org/10.1016/j.jenvman.2023.118690>.

### References

- Aduagna, D., Larsen, L., Lemma, B., Sahilu, G., 2017. Low-cost stormwater filtration system to improve urban water quality: the case of addis ababa, Ethiopia. *J. Water Resour. Protect.* 9 <https://doi.org/10.4236/jwarp.2017.96046>, 06.
- Ahfir, N.-D., Wang, H.Q., Benamar, A., Alem, A., Massei, N., Dupont, J.-P., 2007. Transport and deposition of suspended particles in saturated porous media:

- hydrodynamic effect. *Hydrogeol. J.* 15 (4), 659–668. <https://doi.org/10.1007/s10040-006-0131-3>.
- Ahfir, N.-D., Hammadi, A., Alem, A., Wang, H., Le Bras, G., Ouahbi, T., 2017. Porous media grain size distribution and hydrodynamic forces effects on transport and deposition of suspended particles. *J. Environ. Sci.* 53, 161–172. <https://doi.org/10.1016/j.jes.2016.01.032>.
- Alimi, O.S., Farner Budarz, J., Hernandez, L.M., Tufenkji, N., 2018. Microplastics and nanoplastics in aquatic environments: aggregation, deposition, and enhanced contaminant transport. *Environ. Sci. Technol.* 52 (4), 1704–1724. <https://doi.org/10.1021/acs.est.7b05559>.
- Amelia, T.S.M., Khalik, W.M.A.W.M., Ong, M.C., Shao, Y.T., Pan, H.-J., Bhubalan, K., 2021. Marine microplastics as vectors of major ocean pollutants and its hazards to the marine ecosystem and humans. *Prog. Earth Planet. Sci.* 8 (1), 12. <https://doi.org/10.1186/s40645-020-00405-4>.
- Auta, H.S., Emenike, C.U., Fauziah, S.H., 2017. Distribution and importance of microplastics in the marine environment: a review of the sources, fate, effects, and potential solutions. *Environ. Int.* 102, 165–176. <https://doi.org/10.1016/j.envint.2017.02.013>.
- Benamar, A., Wang, H., Ahfir, N., Alem, A., Massei, N., Dupont, J., 2005. Inertial effects on the transport and the rate deposition of fine particles in a soil. *CR Geosci* 337, 497–504.
- Breiman, L., 1984. *Classification And Regression Trees* (1 St). Routledge. <https://doi.org/10.1201/9781315139470>.
- Chen, Y., Leng, Y., Liu, X., Wang, J., 2020. Microplastic pollution in vegetable farmlands of suburb Wuhan, central China. *Environ. Pollut.* 257, 113449. <https://doi.org/10.1016/j.envpol.2019.113449>.
- Chen, Y., Li, T., Hu, H., Ao, H., Xiong, X., Shi, H., Wu, C., 2021. Transport and fate of microplastics in constructed wetlands: a microcosm study. *J. Hazard Mater.* 415, 125615. <https://doi.org/10.1016/j.jhazmat.2021.125615>.
- Choi, H., Geronimo, F.K.F., Jeon, M., Kim, L.-H., 2021. Investigation of the factors affecting the treatment performance of a stormwater horizontal subsurface flow constructed wetland treating road and parking lot runoff. *Water* 13 (9), 1242. <https://doi.org/10.3390/w13091242>.
- Chrysikopoulos, C.V., Syngouna, V.I., 2014. Effect of gravity on colloid transport through water-saturated columns packed with glass beads: modeling and experiments. *Environ. Sci. Technol.* 48 (12), 6805–6813. <https://doi.org/10.1021/es501295n>.
- Covernton, G.A., Pearce, C.M., Gurney-Smith, H.J., Chastain, S.G., Ross, P.S., Dower, J. F., Dudas, S.E., 2019. Size and shape matter: a preliminary analysis of microplastic sampling technique in seawater studies with implications for ecological risk assessment. *Sci. Total Environ.* 667, 124–132. <https://doi.org/10.1016/j.scitotenv.2019.02.346>.
- Davis, A.P., Hunt, W.F., Traver, R.G., Clar, M., 2009. Bioretention technology: overview of current practice and future needs. *J. Environ. Eng.* 135 (3), 109–117. [https://doi.org/10.1061/\(ASCE\)0733-9372\(2009\)135:3\(109](https://doi.org/10.1061/(ASCE)0733-9372(2009)135:3(109).
- DeNovio, N.M., Saiers, J.E., Ryan, J.N., 2004. Colloid movement in unsaturated porous media: recent advances and future directions. *Vadose Zone J.* 3 (2), 338–351. <https://doi.org/10.2136/vzj2004.0338>.
- Dong, S., Xia, J., Sheng, L., Wang, W., Liu, H., Gao, B., 2021. Transport characteristics of fragmental polyethylene glycol terephthalate (PET) microplastics in porous media under various chemical conditions. *Chemosphere* 276, 130214. <https://doi.org/10.1016/j.chemosphere.2021.130214>.
- Drago, C., Pawlak, J., Weithoff, G., 2020. Biogenic aggregation of small microplastics alters their ingestion by a common freshwater micro-invertebrate. *Front. Environ. Sci.* 8. <https://www.frontiersin.org/articles/10.3389/fenvs.2020.574274>.
- Eitzen, L., Paul, S., Braun, U., Altmann, K., Jekel, M., Ruhl, A.S., 2019. The challenge in preparing particle suspensions for aquatic microplastic research. *Environ. Res.* 168, 490–495. <https://doi.org/10.1016/j.envres.2018.09.008>.
- Enders, K., Lenz, R., Stedmon, C.A., Nielsen, T.G., 2015. Abundance, size and polymer composition of marine microplastics  $\geq 10 \mu\text{m}$  in the Atlantic Ocean and their modelled vertical distribution. *Mar. Pollut. Bull.* 100 (1), 70–81. <https://doi.org/10.1016/j.marpolbul.2015.09.027>.
- Fendall, L.S., Sewell, M.A., 2009. Contributing to marine pollution by washing your face: microplastics in facial cleansers. *Mar. Pollut. Bull.* 58 (8), 1225–1228. <https://doi.org/10.1016/j.marpolbul.2009.04.025>.
- Frey, J., Schmitz, P., Dufreche, J., Gohr Pinheiro, I., 1999. Particle deposition in porous media: analysis of hydrodynamic and weak inertial effects. *Transport Porous Media* 37 (1), 25–54.
- Gatidou, G., Arvaniti, O.S., Stasinakis, A.S., 2019. Review on the occurrence and fate of microplastics in sewage treatment plants. *J. Hazard Mater.* 367, 504–512. <https://doi.org/10.1016/j.jhazmat.2018.12.081>.
- Gilbreath, A., McKee, L., Shimabuku, I., Lin, D., Werbowski, L.M., Zhu, X., Grbic, J., Rochman, C., 2019. Multiyear water quality performance and mass accumulation of PCBs, mercury, methylmercury, copper, and microplastics in a bioretention rain garden. *J. Sustain. Water Built Environ.* 5 (4), 04019004. <https://doi.org/10.1061/JSWBAY.0000883>.
- Gohr, P.I., Schmitz, P., Houi, D., 1999. Particle capture in porous media when physico-chemical effects dominate. *Chem. Eng. Sci.* 54 (17), 3801–3813. [https://doi.org/10.1016/S0009-2509\(98\)00434-5](https://doi.org/10.1016/S0009-2509(98)00434-5).
- Hartmann, N.B., Hüffer, T., Thompson, R.C., Hassellöv, M., Verschoor, A., Dagaard, A. E., Rist, S., Karlsson, T., Brennholt, N., Cole, M., Herrling, M.P., Hess, M.C., Ivleva, N. P., Lusher, A.L., Wagner, M., 2019. Are we speaking the same language? Recommendations for a definition and categorization framework for plastic debris. *Environ. Sci. Technol.* 53 (3), 1039–1047. <https://doi.org/10.1021/acs.est.8b05297>.
- Hatt, B.E., Fletcher, T.D., Deletic, A., 2009. Hydrologic and pollutant removal performance of stormwater biofiltration systems at the field scale. *J. Hydrol.* 365 (3), 310–321. <https://doi.org/10.1016/j.jhydrol.2008.12.001>.
- Hou, J., Xu, X., Lan, L., Miao, L., Xu, Y., You, G., Liu, Z., 2020. Transport behavior of micro polyethylene particles in saturated quartz sand: impacts of input concentration and physicochemical factors. *Environ. Pollut.* 263, 114499. <https://doi.org/10.1016/j.envpol.2020.114499>.
- Hüffer, T., Praetorius, A., Wagner, S., von der Kammer, F., Hofmann, T., 2017. Microplastic exposure assessment in aquatic environments: learning from similarities and differences to engineered nanoparticles. *Environ. Sci. Technol.* 51 (5), 2499–2507. <https://doi.org/10.1021/acs.est.6b04054>.
- Hunt, W.F., Davis, A.P., Traver, R.G., 2012. Meeting hydrologic and water quality goals through targeted bioretention design. *J. Environ. Eng.* 138 (6), 698–707.
- Igalavithana, A.D., Yuan, X., Attanayake, C.P., Wang, S., You, S., Tsang, D.C.W., Nzihou, A., Ok, Y.S., 2022. Sustainable management of plastic wastes in COVID-19 pandemic: the biochar solution. *Environ. Res.* 212, 113495. <https://doi.org/10.1016/j.envres.2022.113495>.
- Kershaw, P., 2016. Marine Plastic Debris and Microplastics—Global Lessons and Research to Inspire Action and Guide Policy Change. <https://doi.org/10.13140/RG.2.2.30493.51687>.
- Koutnik, V.S., Leonard, J., Brar, J., Cao, S., Glasman, J.B., Cowger, W., Ravi, S., Mohanty, S.K., 2022a. Transport of microplastics in stormwater treatment systems under freeze-thaw cycles: critical role of plastic density. *Water Res.* 222, 118950. <https://doi.org/10.1016/j.watres.2022.118950>.
- Koutnik, V.S., Leonard, J., Glasman, J.B., Brar, J., Koydemir, H.C., Novoselov, A., Bertel, R., Tseng, D., Ozcan, A., Ravi, S., Mohanty, S.K., 2022b. Microplastics retained in stormwater control measures: where do they come from and where do they go? *Water Res.* 210, 118008. <https://doi.org/10.1016/j.watres.2021.118008>.
- Kumar, M., Xiong, X., He, M., Tsang, D.C.W., Gupta, J., Khan, E., Harrad, S., Hou, D., Ok, Y.S., Bolan, N.S., 2020. Microplastics as pollutants in agricultural soils. *Environ. Pollut.* 265, 114980. <https://doi.org/10.1016/j.envpol.2020.114980>.
- Kumar, R., Sharma, P., Verma, A., Jha, P.K., Singh, P., Gupta, P.K., Chandra, R., Prasad, P.V.V., 2021. Effect of physical characteristics and hydrodynamic conditions on transport and deposition of microplastics in riverine ecosystem. *Water* 13 (19). <https://doi.org/10.3390/w13192710>.
- Kuoppamäki, K., Pflugmacher Lima, S., Scopetani, C., Setälä, H., 2021. The ability of selected filter materials in removing nutrients, metals, and microplastics from stormwater in biofilter structures. *J. Environ. Qual.* 50 (2), 465–475. <https://doi.org/10.1002/jeq2.20201>.
- Lange, K., Magnusson, K., Viklander, M., Blecken, G.-T., 2021. Removal of rubber, bitumen and other microplastic particles from stormwater by a gross pollutant trap—bioretention treatment train. *Water Res.* 202, 117457. <https://doi.org/10.1016/j.watres.2021.117457>.
- Lange, K., Österlund, H., Viklander, M., Blecken, G.-T., 2022. Occurrence and concentration of 20–100  $\mu\text{m}$  sized microplastic in highway runoff and its removal in a gross pollutant trap – bioretention and sand filter stormwater treatment train. *Sci. Total Environ.* 809, 151151. <https://doi.org/10.1016/j.scitotenv.2021.151151>.
- Larsson, R., 2008. *Jords Egenskaper*.
- Liu, F., Olesen, K.B., Borregaard, A.R., Vollertsen, J., 2019. Microplastics in urban and highway stormwater retention ponds. *Sci. Total Environ.* 671, 992–1000. <https://doi.org/10.1016/j.scitotenv.2019.03.416>.
- Löder, M.G.J., Kuczerka, M., Mintenig, S., Lorenz, C., Gerdt, G., 2015. Focal plane array detector-based micro-Fourier-transform infrared imaging for the analysis of microplastics in environmental samples. *Environ. Chem.* 12 (5), 563–581. <https://doi.org/10.1071/EN14205>.
- Long, M., Paul-Pont, I., Hegaret, H., Moriceau, B., Lambert, C., Huvet, A., Soudant, P., 2017. Interactions between polystyrene microplastics and marine phytoplankton lead to species-specific heteroaggregation. *Environ. Pollut.* 228, 454–463. <https://doi.org/10.1016/j.envpol.2017.05.047>.
- Lusher, A.L., Bråte, L.L.N., Munno, K., Hurley, R.R., Welden, N.A., 2020. Is it or isn't it: the importance of visual classification in microplastic characterization. *Appl. Spectrosc.* 74 (9), 1139–1153. <https://doi.org/10.1177/0003702820930733>.
- Martínez Silva, P., Nanny, M.A., 2020. Impact of microplastic fibers from the degradation of nonwoven synthetic textiles to the Magdalena river water column and river sediments by the city of Neiva, Huila (Colombia). *Water* 12 (4). <https://doi.org/10.3390/w12041210>.
- Masura, J., Baker, J.E., Foster, G.D., Gregory, D., Arthur, C., Herring, C., 2015. Laboratory methods for the analysis of microplastics in the marine environment: recommendations for quantifying synthetic particles in waters and sediments (noaa: 10296), 1959-. <https://repository.library.noaa.gov/view/noaa/10296>.
- Mintenig, S.M., Int-Veen, I., Löder, M.G.J., Primpke, S., Gerdt, G., 2017. Identification of microplastic in effluents of waste water treatment plants using focal plane array-based micro-Fourier-transform infrared imaging. *Water Res.* 108, 365–372. <https://doi.org/10.1016/j.watres.2016.11.015>.
- Mohamed Nor, N.H., Obbard, J.P., 2014. Microplastics in Singapore's coastal mangrove ecosystems. *Mar. Pollut. Bull.* 79 (1), 278–283. <https://doi.org/10.1016/j.marpolbul.2013.11.025>.
- Molazadeh, M., Liu, F., Simon-Sánchez, L., Vollersten, J., 2023. Buoyant microplastics in freshwater sediments – how do they get there? *Sci. Total Environ.* 860, 160489. <https://doi.org/10.1016/j.scitotenv.2022.160489>.
- Morash, J., Wright, A., LeBleu, C., Meder, A., Kessler, R., Brantley, E., Howe, J., 2019. Increasing sustainability of residential areas using rain gardens to improve pollutant capture, biodiversity and ecosystem resilience. *Sustainability* 11 (12). <https://doi.org/10.3390/su11123269>.
- Nkwonta, O., 2010. A comparison of horizontal roughing filters and vertical roughing filters in wastewater treatment using gravel as a filter media. *Int. J. Phys. Sci.* 5, 1240–1247.
- Olesen, K.B., Stephansen, D.A., van Alst, N., Vollertsen, J., 2019. Microplastics in a stormwater pond. *Water* 11 (7). <https://doi.org/10.3390/w11071466>.

- Österlund, H., Blecken, G., Lange, K., Marsalek, J., Gopinath, K., Viklander, M., 2023. Microplastics in urban catchments: review of sources, pathways, and entry into stormwater. *Sci. Total Environ.* 858, 159781 <https://doi.org/10.1016/j.scitotenv.2022.159781>.
- O'Connor, D., Pan, S., Shen, Z., Song, Y., Jin, Y., Wu, W.-M., Hou, D., 2019. Microplastics undergo accelerated vertical migration in sand soil due to small size and wet-dry cycles. *Environ. Pollut.* 249, 527–534. <https://doi.org/10.1016/j.envpol.2019.03.092>.
- Payne, E., Hatt, B., Deletic, A., Dobbie, M., McCarthy, D., Chandrasena, G., 2015. *Adoption Guidelines For Stormwater Biofiltration Systems*. Cooperative Research Centre for Water Sensitive Cities. [www.watersensitivecities.org.au](http://www.watersensitivecities.org.au).
- Porubcan, A.A., Xu, S., 2011. Colloid straining within saturated heterogeneous porous media. *Water Res.* 45 (4), 1796–1806. <https://doi.org/10.1016/j.watres.2010.11.037>.
- Primpke, S., Lorenz, C., Rascher-Friesenhausen, R., Gerdt, G., 2017. An automated approach for microplastics analysis using focal plane array (FPA) FTIR microscopy and image analysis. *Anal. Methods* 9 (9), 1499–1511. <https://doi.org/10.1039/C6AY02476A>.
- Primpke, S., Wirth, M., Lorenz, C., Gerdt, G., 2018. Reference database design for the automated analysis of microplastic samples based on Fourier transform infrared (FTIR) spectroscopy. *Anal. Bioanal. Chem.* 410 (21), 5131–5141. <https://doi.org/10.1007/s00216-018-1156-x>.
- Primpke, S., Cross, R.K., Mintenig, S.M., Simon, M., Vianello, A., Gerdt, G., Vollertsen, J., 2020. Toward the systematic identification of microplastics in the environment: evaluation of a new independent software tool (siMPle) for spectroscopic analysis. *Appl. Spectrosc.* 74 (9), 1127–1138. <https://doi.org/10.1177/0003702820917760>.
- Rasmussen, L.A., Iordachescu, L., Tumlin, S., Vollertsen, J., 2021. A complete mass balance for plastics in a wastewater treatment plant—macroplastics contributes more than microplastics. *Water Res.* 201, 117307 <https://doi.org/10.1016/j.watres.2021.117307>.
- Rhein, F., Nirschl, H., Kaegi, R., 2022. Separation of microplastic particles from sewage sludge extracts using magnetic seeded filtration. *Water Res.* X 17, 100155. <https://doi.org/10.1016/j.wroa.2022.100155>.
- Rokach, L., Maimon, O., 2005. Decision trees. *The Data Mining and Knowledge Discovery Handbook* 6, 165–192. [https://doi.org/10.1007/0-387-25465-X\\_9](https://doi.org/10.1007/0-387-25465-X_9).
- Sakthivadivel, R., University of California, Berkeley, 1969. Clogging of a granular porous medium by sediment. In: *Hydraulic Engineering Laboratory*. University of California, College of Engineering. <https://catalog.hathitrust.org/Record/100801498>.
- Samuel, M.P., Senthilvel, S., Tamilmani, D., Mathew, A.C., 2012. Performance evaluation and modelling studies of gravel-coir fibre-sand multimedia stormwater filter. *Environ. Technol.* 33 (17), 2057–2069. <https://doi.org/10.1080/09593330.2012.660642>.
- Sembling, E., Fajar, M., Handajani, M., 2021. Performance of rapid sand filter – single media to remove microplastics. *Water Supply* 21 (5), 2273–2284. <https://doi.org/10.2166/ws.2021.060>.
- Simon, M., van Alst, N., Vollertsen, J., 2018. Quantification of microplastic mass and removal rates at wastewater treatment plants applying Focal Plane Array (FPA)-based Fourier Transform Infrared (FT-IR) imaging. *Water Res.* 142, 1–9. <https://doi.org/10.1016/j.watres.2018.05.019>.
- Smyth, K., Drake, J., Li, Y., Rochman, C., Van Seters, T., Passeport, E., 2021. Bioretention cells remove microplastics from urban stormwater. *Water Res.* 191, 116785 <https://doi.org/10.1016/j.watres.2020.116785>.
- Tagg, A.S., Sapp, M., Harrison, J.P., Ojeda, J.J., 2015. Identification and quantification of microplastics in wastewater using focal plane array-based reflectance micro-FT-IR imaging. *Anal. Chem.* 87 (12), 6032–6040. <https://doi.org/10.1021/acs.analchem.5b00495>.
- Tagg, A.S., Sapp, M., Harrison, J.P., Sinclair, C.J., Bradley, E., Ju-Nam, Y., Ojeda, J.J., 2020. Microplastic monitoring at different stages in a wastewater treatment plant using reflectance micro-FTIR imaging. *Front. Environ. Sci.* 8. <https://www.frontiersin.org/articles/10.3389/fenvs.2020.00145>.
- Talvitie, J., Mikola, A., Koistinen, A., Setälä, O., 2017. Solutions to microplastic pollution—Removal of microplastics from wastewater effluent with advanced wastewater treatment technologies. *Water Res.* 123, 401–407. <https://doi.org/10.1016/j.watres.2017.07.005>.
- Thompson, R.C., Olsen, Y., Mitchell, R.P., Davis, A., Rowland, S.J., John, A.W.G., McGonigle, D., Russell, A.E., 2004. Lost at sea: where is all the plastic? *Science* 304 (5672). <https://doi.org/10.1126/science.1094559>, 838–838.
- Tirpak, R.A., Afroz, A.N., Winston, R.J., Valença, R., Schiff, K., Mohanty, S.K., 2021. Conventional and amended bioretention soil media for targeted pollutant treatment: a critical review to guide the state of the practice. *Water Res.* 189, 116648 <https://doi.org/10.1016/j.watres.2020.116648>.
- Tumwet, F.C., Serbe, R., Kleint, T., Scheytt, T., 2022. Effect of fragmentation on the transport of polyvinyl chloride and low-density polyethylene in saturated quartz sand. *Sci. Total Environ.* 836, 155657 <https://doi.org/10.1016/j.scitotenv.2022.155657>.
- Vianello, A., Jensen, R.L., Liu, L., Vollertsen, J., 2019. Simulating human exposure to indoor airborne microplastics using a Breathing Thermal Manikin. *Sci. Rep.* 9 (1), 8670. <https://doi.org/10.1038/s41598-019-45054-w>.
- Vinay, Surana, D., Ghosh, P., Kumar, M., Varjani, S., Kumar, V., Mannina, G., 2023. Contemporary drift in emerging micro(nano)plastics removal and upcycling technologies from municipal wastewater sludge: strategic innovations and prospects. *Current Pollution Reports* 9 (2), 174–197. <https://doi.org/10.1007/s40726-023-00261-y>.
- Wang, X., Bolan, N., Tsang, D.C.W., Sarkar, B., Bradney, L., Li, Y., 2021. A review of microplastics aggregation in aquatic environment: influence factors, analytical methods, and environmental implications. *J. Hazard Mater.* 402, 123496 <https://doi.org/10.1016/j.jhazmat.2020.123496>.
- Werbowski, L.M., Gilbreath, A.N., Munno, K., Zhu, X., Grbic, J., Wu, T., Sutton, R., Sedlak, M.D., Deshpande, A.D., Rochman, C.M., 2021. Urban stormwater runoff: a major pathway for anthropogenic particles, black rubbery fragments, and other types of microplastics to urban receiving waters. *ACS ES&T Water* 1 (6), 1420–1428. <https://doi.org/10.1021/acsestwater.1c00017>.
- Windsor, F.M., Tilley, R.M., Tyler, C.R., Ormerod, S.J., 2019. Microplastic ingestion by riverine macroinvertebrates. *Sci. Total Environ.* 646, 68–74. <https://doi.org/10.1016/j.scitotenv.2018.07.271>.
- Yano, K., Geronimo, F., Reyes, N., Kim, L., 2021. Characterization and Comparison of Microplastic Occurrence in Point and Non-point Pollution Sources, vol. 797. *SCIENCE OF THE TOTAL ENVIRONMENT*. <https://doi.org/10.1016/j.scitotenv.2021.148939>.
- Yao, K.-M., Habibian, M.T., O'Melia, C.R., 1971. Water and waste water filtration. *Concepts and applications. Environ. Sci. Technol.* 5 (11), 1105–1112.
- Yantsios, S.G., Karabelas, A.J., 2003. Deposition of micron-sized particles on flat surfaces: effects of hydrodynamic and physicochemical conditions on particle attachment efficiency. *Chem. Eng. Sci.* 58 (14), 3105–3113. [https://doi.org/10.1016/S0009-2509\(03\)00169-6](https://doi.org/10.1016/S0009-2509(03)00169-6).
- Zhang, W., 2014. Nanoparticle aggregation: principles and modeling. *Nanomaterials* 811, 19–43. [https://doi.org/10.1007/978-94-017-8739-0\\_2](https://doi.org/10.1007/978-94-017-8739-0_2).
- Zhang, X., Chen, Y., Li, X., Zhang, Y., Gao, W., Jiang, J., Mo, A., He, D., 2022. Size/shape-dependent migration of microplastics in agricultural soil under simulative and natural rainfall. *Sci. Total Environ.* 815, 152507 <https://doi.org/10.1016/j.scitotenv.2021.152507>.